

# Short Range Radar Based on UWB Technology

L. Sakkila<sup>1,2,3</sup>, C. Tatkeu<sup>1,2</sup>, Y. ElHillali<sup>1,3</sup>, A. Rivenq<sup>1,3</sup>,  
F. ElBahhar<sup>1,2</sup> and J-M. Rouvaen<sup>1,3</sup>

<sup>1</sup>*Univ. Lille Nord de France, F-59000 Lille,*

<sup>2</sup>*INRETS, LEOST, F-59666 Villeneuve d'Ascq,*

<sup>3</sup>*UVHC, IEMN-DOAE, F-59313 Valenciennes,  
France*

## 1. Introduction

In this Chapter, a short range radar system based on ultra-wideband (UWB) technology is presented. The radar and its applications were reserved during a long time to national defence, air security or weather services domains. Since a few years, with the emergence of new technologies, the radar applications were developed and become known in many sectors of daily life. The arrival of a new technology called Ultra-Wideband (UWB) allows in particular the development of compact and low-cost radar with multiple fields of applications. UWB uses very short non-sinusoidal pulses that have widths less than 1.5 ns, so that the spectrum of the transmitted signals may spread over several Gigahertz. This radar offers a resolution in distance of about a few centimetres, for example 15 cm for a pulse width of 1ns, making this system very interesting in several short range applications. UWB radar has many applications in Medical, Building, Surveillance, Security and Monitoring applications [Dam2007] and will appear more and more in our daily life. For example, UWB radar systems for local monitoring allow creating dome radar surveillance around a sensitive object or subject. These compact systems contain a small UWB radar with a range of about 10 meters, a standard radio system for transmitting the alarm in case of intrusion and a GPS system for localisation function. These systems can be engaged in public safety functions in buildings, aircrafts or for artwork protection in a museum, but also as an alarm system around a house or near a swimming pool to avoid too frequent small children drowning. Thanks to their sensitivity the UWB radar can detect movement as slight as a heart beat or breathing rate. These systems is responsive enough to accurately depict a heart rate as compared to others existing systems. UWB radar could be used as ground penetrating radar (GPR). GPR systems can obtain very precise and detailed images sub-soil. UWB radar is moved along surface and sends electromagnetic pulses into the ground. The analysis of received echoes can produce a very specific profile of underground. The investigation depth varies, depending on the type of ground, from a few meters in asphalt or clay to more than a hundred meters in limestone or granite, or even several kilometres into the ice. Finally, UWB radar could be used for short range collision avoidance as mentioned in this paper.

This collision avoidance system, 24 GHz UWB Short Range Radar (SRR), was developed principally by European car manufacturers. It is a combination of an UWB radar and a

conventional Doppler radar to measure vehicle speeds and to detect obstacles with a resolution in distance between 10 cm and 30 m. These systems are placed at the front and sides of the vehicle and warn the driver of potential impacts with other vehicles or pedestrians. They are also useful as parking assistance. Current systems warn the driver of a potential danger without intervening in the braking system. This system should allow a reduction in traffic accidents as the standard rear collisions often due to inattention, so these collisions, estimated 88%, could be avoided [ESaf2006].

In the following paragraphs, UWB technology, its advantages and disadvantages will be introduced, before presenting the UWB radar.

## 2. Ultra Wide Band technology

The radar studied exploits a new radio frequency technique called Ultra-Wide Band (UWB), to perform obstacles detection. The UWB technology is a radio modulation technique based on very short pulses transmission [Bar2000].

These pulses have typical widths of less than 1.5 ns and thus bandwidths over 1 GHz. This technique, as defined by the Federal Communication Commission (FCC) [Fcc2002], has a Fractional Bandwidth (FB) greater than 25%, this fractional bandwidth is defined as:

$$FB = \frac{\text{signal bandwidth}}{\text{center frequency}} = \frac{f_h - f_l}{f_h + f_l} * 100 \quad (1)$$

where  $f_h$  and  $f_l$  represent respectively the highest and the lowest frequencies which are 10 dB below the maximum.

The key value of UWB is that its RF (Radio Frequency) bandwidth is significantly wider than the information bandwidth [Fcc2000].

The advantages of UWB technology are:

- Its exceptional multipath immunity.
- Its relative simplicity and likely lower cost to build than spread spectrum radios.
- Its substantially low consumed power, lower than existing conventional radios.
- Its implementation as a simple integrated circuit chipset with very few off-chip parts.
- Its high bandwidth capacity and multi-channel performance.
- Its high data rates for wireless communications.

However, UWB technology presents also some disadvantages among which are:

- A risk of being subjected to the dispersion and frequency distortion phenomena since they extend over a wide bandwidth [Tay1995]. Dispersion is the phenomenon whereby different frequency components of a signal do not propagate at the same speed in a channel. The distortion in frequency can be defined as non-uniform attenuation of different frequency components of a signal. UWB systems must therefore take account of these effects.
- Throughput performance will probably never exceed that of the optical systems at great rates

Moreover, thanks to advantages provided by this technology, the UWB radar presents good precision in distance calculation. Below, the principle of UWB radar and its benefits are introduced.

### 3. UWB radar

UWB radar sends very short electromagnetic pulses. This type of radar can employ traditional UWB waveforms such as Gaussian or monocycle pulses. To calculate the distance between radar and obstacle, the time delay  $\Delta t$  between emission and reception is measured. This distance is given by:

$$d = \frac{c \cdot \Delta t}{2} \quad (2)$$

where  $c$  is the light speed.

This radar offers a resolution in distance of about 15 cm for a width pulse of 1ns, so that this system is very interesting for short range road safety applications.

This UWB radar presents good performances, so as firstly, the brevity of the pulses with strong spectral contents makes it possible to obtain information on the target with a rich transitory response content. This allows the dissociation of various echoes at the reception stage. Then the broad band spectrum authorizes to obtain results on the entire frequency band in a single measurement together with a strong capacity of detection. Finally the pulse spectrum has capabilities to penetrate through naturally screening materials (ground, vegetation...) [Dam2007].

Considering all these properties, UWB radar, using very short pulses, is of great interest for many applications of obstacle detection and target identification in the short range.

This UWB radar is operational for the short ranges where the conventional radars, using pulses of width from 1 $\mu$ s, are unable to detect obstacles below 15 meters. Moreover, these is not an intermediate electronic stage because of the non-existence of the carrier frequency. So, this system has a simpler implementation and lower cost compared to the traditional radar.

According to the application considered, the choice of the appropriate UWB waveform needed. In fact, each waveform gives a specific cross-correlation function and the obtained peaks of this function must be easily detectable at the receiver.

Different waveforms can be used for the UWB radar [Cham1992] for example: Gaussian pulse, monocycle pulse, Gegenbauer and Hermite functions.

### 4. UWB pulse radio

#### 4.1 Gaussian pulse

The Gaussian pulse is a waveform described by the Gaussian distribution.

In the time domain, the expression of the Gaussian pulse waveform is given by [Bar2000]:

$$g(t) = A \exp[-(t / \sigma)^2] \quad (3)$$

where  $A$  stands for the maximum amplitude and  $\sigma$  for the width of the Gaussian pulse. The corresponding time and spectral representations are given in figure 1 assuming a sampling frequency of 20 GHz/Samples.

#### 4.2 Monocycle pulse

The monocycle pulse is the first derivative of the Gaussian pulse. The expression for the monocycle pulse waveform is written as [Carl2000]

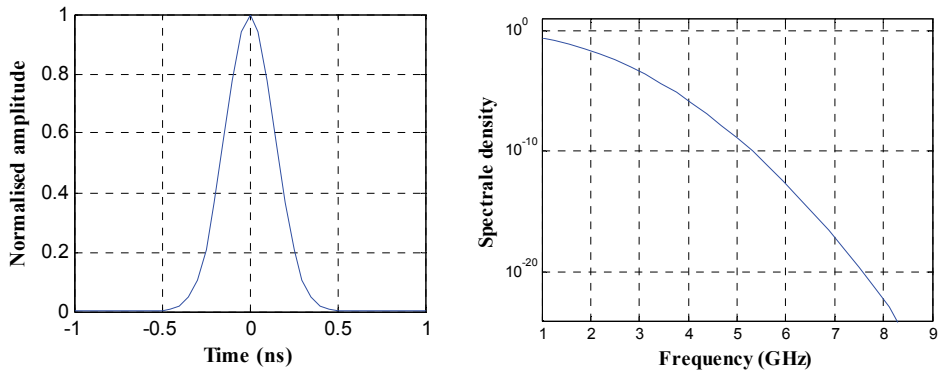


Fig. 1. Gaussian pulse time and spectral representations.

$$m(t) = \frac{t}{\tau} \exp[-(t / \tau)^2] \tag{4}$$

where  $\tau$  is the pulse width (the centre frequency is then proportional to  $1/ \tau$ ).

The time and spectral representations are given in figure 2, again with a sampling frequency of 20GHz/Samples.

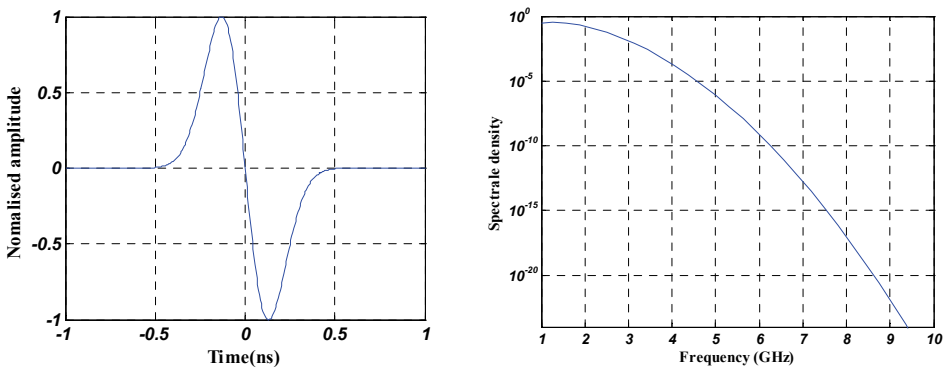


Fig. 2. Monocycle pulse time and frequency representations.

The  $n^{th}$  derivate of Gaussian pulse can be obtained from the following expression:

$$p^n(t) = -\frac{n-1}{\sigma^2} g^{(n-2)}(t) - \frac{t}{\sigma^2} g^{(n-1)}(t)$$

In the simple case, single user or single radar system, the configuration of transmitter and receiver is given by the figure 3. So, due to the fact that Gaussian and its first derivate Monocycle pulses are easy to generate, they allow very simple and less expensive implementation of a radar in a single user case. The pulse leaving the generator is transmitted using the transmitter antenna. After reflection on the obstacle, the received signal echo is correlated with the reference pulse, in order to detect the peak, by using the threshold detection method.

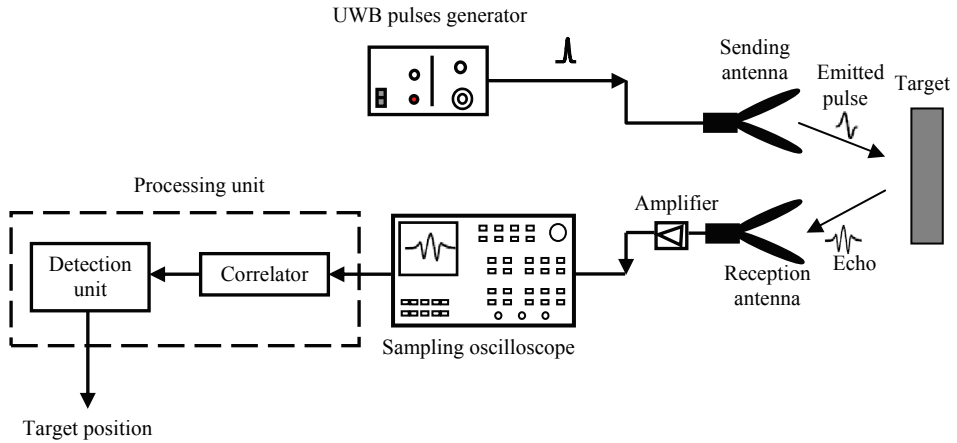


Fig. 3. The radar based on UWB pulses.

However, in a real scenario, several UWB radars may exist in the same propagation channel (environment). So, using these simple waveforms (Gaussian and Monocycle pulses), is not appropriate. In fact, it is necessary to encode the pulses emitted by different users in order to avoid interference between them. To do this, to each user or radar system a specific code is attributed. The coding is done by multiplying each bit of code by the UWB pulse as in CDMA (Code Division Multiple Access) technique (Figure 4).

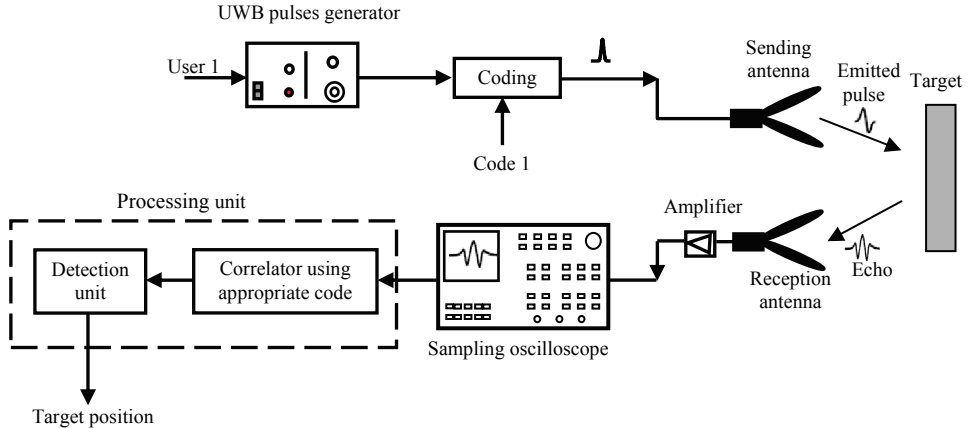


Fig. 4. The proposed radar based on UWB coded pulse.

Another way to perform multiple access exists; namely using waveforms based on orthogonal polynomials. Some UWB orthogonal waveforms, such as Gegenbauer and Hermite polynomials, could be used to ensure multiple access (each user has his own order of polynomial waveform) without resorting to the use of codes, which can reduce the complexity of the system compared with conventional systems. Multiple access based on the use of unique waveforms allows for up to 8 users.

### 4.3 Orthogonal waveforms for UWB radar system

#### 4.3.1 Gegenbauer polynomials

The Gegenbauer polynomials are also called ultra-spherical polynomials. These polynomials are defined in the interval  $[-1, 1]$  and they satisfy the following differential equation of second order [Elb2005]:

$$(1-x^2)G''(n, \beta, x) - (2\beta+2)xG'_n(x) - n(n+2\beta+2)G_n(x) = 0 \quad (5)$$

with  $\beta > -1/2$

$n$ : order of Gegenbauer polynomial

The different orders of the Gegenbauer polynomials are bound by the following recurrence equation:

$$G(n, \beta, x) = 2 \left( 1 + \frac{n+\beta-1}{n} \right) x G(n-1, \beta, x) - \left( 1 + \frac{n+2\beta-2}{n} \right) G(n-2, \beta) \quad (6)$$

for  $n > 1$

The weight function for these polynomials is given by:

$$w(x, \beta) = (1-x^2)^{\beta-1/2} \quad (7)$$

To be able to use these polynomials in an UWB communication system, the signals generated from polynomials must be very short. So, the orders of polynomials  $G(n, \beta, x)$  are multiplied by a factor corresponding to the square root of the weight function of this polynomials family [Elb2005]. In general we have following:

$$\int w(x, \beta) G(m, \beta, x) G(n, \beta, x) = 0 \quad (8)$$

The modified Gegenbauer function is given by the following equation:

$$G_u(n, \beta, x) = \sqrt{w(x, \beta)} * G(n, \beta, x) \quad (9)$$

The first four orders of these functions for  $\beta = 1$  are given by the following expressions:

$$\begin{aligned} G_u(0, \beta, x) &= 1 * (1-x^2)^{1/4} \\ G_u(1, \beta, x) &= 2x * (1-x^2)^{1/4} \\ G_u(2, \beta, x) &= (-1+4x^2) * (1-x^2)^{1/4} \\ G_u(3, \beta, x) &= (-4x+8x^3) * (1-x^2)^{1/4} \end{aligned} \quad (10)$$

Figure 5 illustrates the time representation of the first four orders of modified Gegenbauer functions with  $\beta = 1$ .

The spectral representation is given in figure 6.

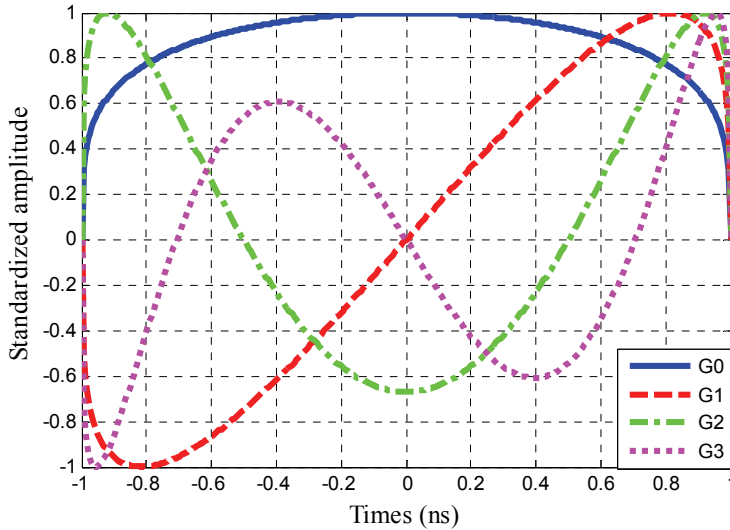


Fig. 5. Modified Gegenbauer functions of orders  $n = 0, 1, 2$  and  $3$ .

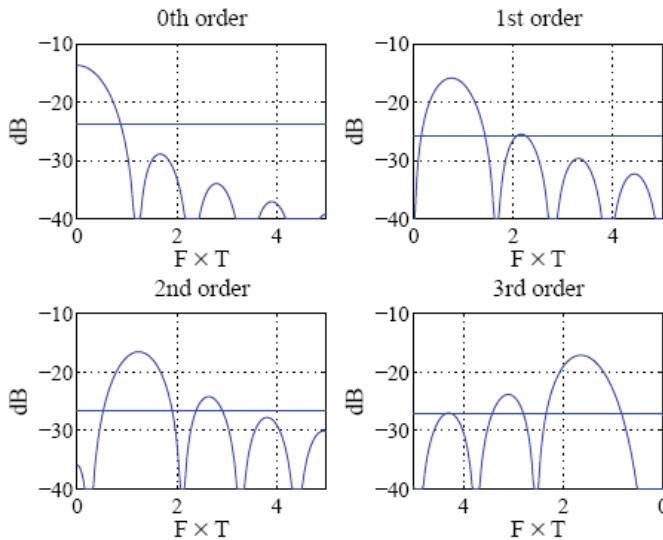


Fig. 6. Spectral representation for modified Gegenbauer functions of orders  $n = 0$  to  $3$ .

**4.3.2 The modified Hermite functions**

Ghavami, Michael and Kohno have proposed the Modified Hermite functions for a multi-user communication system [Lach2002]. These functions are defined in the interval  $[-\infty, +\infty]$  by:

$$h_{e0}(t) = 1 \tag{11}$$

$$h_{e_n}(t) = (-1)^n e^{t^2/4} \frac{d^n}{dt^n} (e^{-t^2/2}) \quad (12)$$

where  $n = 1, 2, \dots$ ,  $n$  represents the order.

Different orders of Hermite polynomials are associated by the following equations

$$h_{e_{n+1}}(t) = t h_{e_n}(t) - \dot{h}_{e_n}(t) \quad (13)$$

$$\dot{h}_{e_n}(t) = n h_{e_{n-1}}(t) \quad (14)$$

with  $\dot{h}$  present the derivative of  $h$

Using equations (13) and (14), the Hermite polynomials satisfy the differential equation of second order defined as:

$$\ddot{h}_{e_n} - t \dot{h}_{e_n} + n h_{e_n} = 0 \quad (15)$$

The Hermite functions are derived from these polynomials by multiplying them by the factor  $e^{-t^2/4}$  as follows:

$$\begin{aligned} h_n(t) &= e^{-t^2/4} h_{e_n}(t) \\ &= (-1)^n e^{-t^2/4} \frac{d^n}{dt^n} (e^{t^2/2}) \end{aligned} \quad (16)$$

Therefore, the orthogonal Hermite functions must verify the following differential equations:

$$\ddot{h}_n + (n + \frac{1}{2} - \frac{1}{4}t^2) h_n = 0 \quad (17)$$

$$\dot{h}_n + \frac{t}{2} h_n = n h_{n-1} \quad (18)$$

$$h_{n+1} = \frac{t}{2} h_n - \dot{h}_n \quad (19)$$

If the Fourier transform of  $h_n(t)$  is symbolized by  $H_n(f)$ , equations (17), (18) and (19) can be written respectively, as follows:

$$\ddot{H}_n + 16\pi^2 (n + \frac{1}{2} - 4\pi^2 f^2) H_n = 0 \quad (20)$$

$$j8\pi^2 f H_n + j \dot{H}_n = 4\pi n H_{n-1} \quad (21)$$

$$H_{n+1} = j \frac{1}{4\pi} \dot{H}_n - j2\pi f H_n \quad (22)$$

For example, for  $n=0$ ,  $h_0(t) = e^{-t^2/4}$  and  $H_0(f) = 2\sqrt{\pi} e^{-4\pi^2 f^2}$ , all other orders can be found. The first three orders, after the order 0, are given by the following equation:

$$\begin{aligned} H_1(f) &= (-4j\pi f)^2 \sqrt{\pi} e^{-4\pi^2 f^2} \\ H_2(f) &= (1 - 16\pi^2 f^2)^2 \sqrt{\pi} e^{-4\pi^2 f^2} \\ H_3(f) &= (-12j\pi f + 64j\pi^3 f^3)^2 \sqrt{\pi} e^{-4\pi^2 f^2} \end{aligned} \quad (23)$$

The first four Hermite time functions ( $n = 0$  to 3), presented in Figure 7, are given by equations:

$$\begin{aligned} h_0(t) &= e^{-t^2/4} \\ h_1(t) &= te^{-t^2/4} \\ h_2(t) &= (t^2 - 1)e^{-t^2/4} \\ h_3(t) &= (t^3 - 3t)e^{-t^2/4} \end{aligned} \quad (24)$$

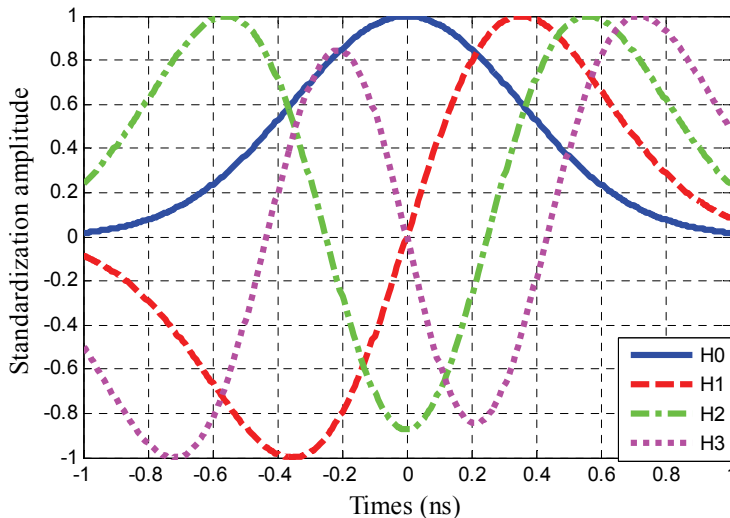


Fig. 7. Hermite functions, orders  $n = 0$  to 3.

Their widths are normalized to 1 ns, the truncation being performed so that at least 99% of energy is kept for the fourth order function. The vertical units are chosen so that the energy of all functions is equal to unity.

The spectral representation is given in figure 8.

The realization of an UWB radar system requires the choice of the waveform. A good choice of this parameter allows optimisation of performances at the reception stage [Elb2001] and reduces the implementation complexity. In order to choose the most appropriate waveform

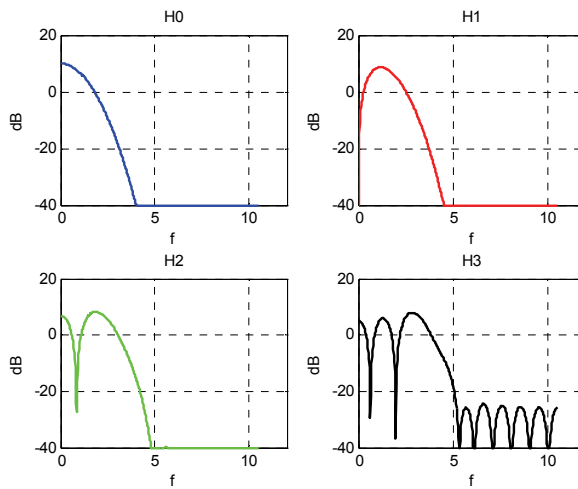


Fig. 8. Spectral representation for Hermite functions of orders  $n = 0$  to 3.

for the radar function, in the following paragraphs, the autocorrelation functions of different waveforms are compared in simulations first and then using the real signals.

At each step, a comparison is made at first between the autocorrelation functions, in terms of dynamics (difference between the correlation peak amplitude and the maximum amplitude of noise), peak width measured at  $-3\text{dB}$  and a new criterion that represents the ratio between the dynamics and the peak width. Using this criterion we consider that the higher this ratio, the better will be the performances of the radar. The ratio between the dynamics and peak width of different orders of Gegenbauer and Hermite polynomials will be compared. The orders that give the best performance for the radar detection functionality is chosen, so the best ratio between the dynamics and peak width, and compared those selected with the Gaussian and monocycle pulses autocorrelation functions.

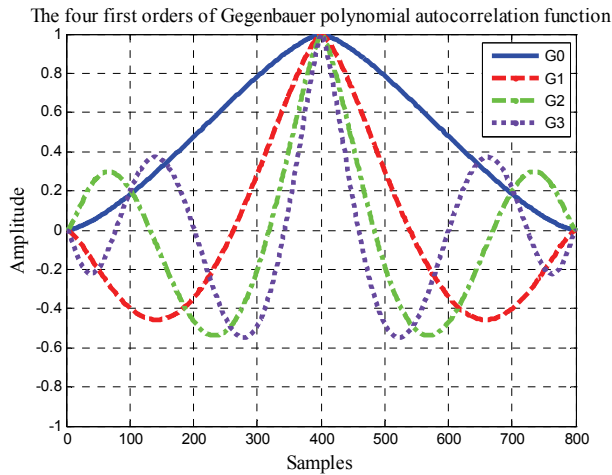
## 5. Comparison performances of UWB waveforms

The autocorrelation functions of different orders Gegenbauer functions are given in figure 9. The comparison between these functions is given in table 1. We can see that the highest ratio between dynamic and peak width belongs to the order 3 autocorrelation of Gegenbauer polynomials.

The same comparison is made for the Hermite polynomials. Results are shown in figure 10. The best autocorrelation is obtained with order 1 of Hermite function H1.

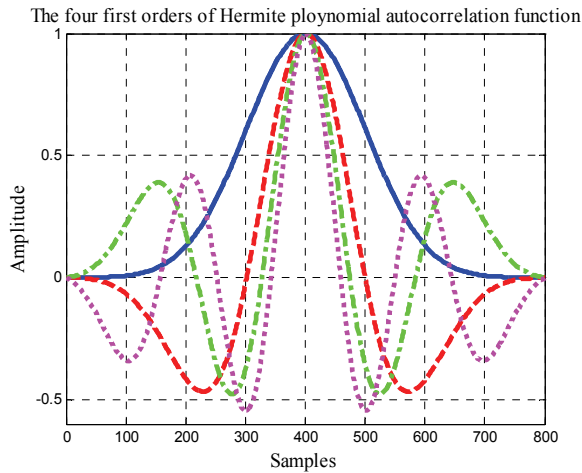
Then, a comparison between the orders of the Gegenbauer and Hermite functions chosen and the Gaussians and Monocycle pulses is made. The functions that offer the best autocorrelations is sought.

Considering the ratio between dynamics and the correlation peak width, the order 3 of Gegenbauer function followed by the monocycle pulse and the order 1 of Hermite function are better. In addition, taking the realisation complexity into account, monocycle offers advantages over other waveforms. So Monocycle pulse compared to order 1 of Hermite function, order 3 of Gegenbauer function and Gaussian pulse seems more adapted for our system in single-user case. However, all these waveforms are interesting in multi-users case.



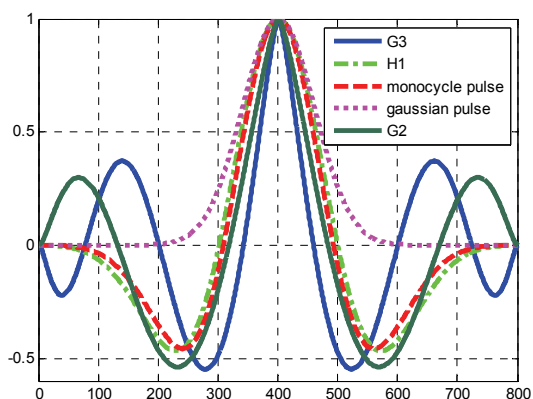
Waveform	Dynamics (D)	Peak width (W)	Ratio (D/W)
G0	1	386	$26.10^{-4}$
G1	1	150	$67.10^{-4}$
G2	0,7	89	$79.10^{-4}$
G3	0,63	62	$102.10^{-4}$

Fig. 9. Comparison between autocorrelation functions of the first four orders of Gegenbauer functions.



Waveform	Dynamics (D)	Peak width (W)	Ratio (D/W)
H0	1	234	$43.10^{-4}$
H1	1	124	$81.10^{-4}$
H2	0,61	94	$65.10^{-4}$
H3	0,58	74	$78.10^{-4}$

Fig. 10. Comparison between autocorrelation functions of the first four orders of Hermite functions.



Waveform	Dynamics (D)	Peak width (W)	Ratio (D/W)
H1	1	124	$81.10^{-4}$
G2	0,7	89	$79.10^{-4}$
G3	0,63	62	$102.10^{-4}$
Monocycle pulse	1	115	$87.10^{-4}$
Gaussian pulse	1	142	$70.10^{-4}$

Fig. 11. Comparison of G2, G3, H1, and Gaussian and Monocycle pulses autocorrelation functions.

In order to validate the simulation results and compare between different waveforms, some tests are performed in an anechoic chamber in order to isolate the effects of the equipment from that of noise. A UWB pulse generator launches waveforms with a sampling frequency of 20 GS/sec. The receiver includes an amplifier and a direct sampling analyzer with 12 GHz bandwidth, 40GS/sec sampling rate and 8 bits precision. Two "Vivaldi" antennas are used for measurements, one for emission and the other for reception.

For experimental comparisons of waveforms, signals used correspond to the signals taken in the absence of target; they therefore correspond to the leakage between the antennas for transmission and reception.

The same comparisons, as in simulations, are made and experimental results confirm the simulations results.

## 6. UWB System for avoidance collision applications

To evaluate radar performances based on UWB technology in outdoor environment, a mock-up laboratory has been developed as described above and several tests, in real conditions, were realized in different configurations using different obstacles (Car, pedestrian, metal plate of dimension 1 squared meter, wooden plate, motorway barrier...). To determine the target position, the received signal is correlated with reference signal and position is then calculated by the threshold detection method.

UWB radar has been implemented using a monocycle pulse generator. It generates monocycle pulses of 3V peak to peak amplitude and 300 ps width. The pulse leaving the generator is transmitted using the transmitter antenna, this emitted signal of duration T is

noted  $s(t)$ . After reflection on the obstacle, the received signal  $r(t)$  is correlated with the reference pulse  $c(t)$ .

The received signal is given by the formula:

$$r(t) = A.s(t - \tau) + n(t) \quad (25)$$

where  $n(t)$  is the noise

$\tau$  : delay time

The most probable positions are those that make up the following expression:

$$R_{rc} = \int_0^T r(t)c(t)dt \quad (26)$$

This expression is nothing other than the correlation of the received signal with the reference. The value of this expression represents the possibility of the presence of the obstacle and maxima correspond to the most probable positions of the target. These maxima are detected using the method of threshold detection

The measurements have been performed using the monocycle pulse. In figure 12, the reference signal  $c(t)$  is presented. It is the monocycle pulse deformed successively first by the transmitter antenna and after by the receiver one, this signal is called here  $c(t)$ . The pulse time sampling is  $8.33 \cdot 10^{-12}$ s.

## 7. Test instrumentation

### 7.1 Single obstacle detection case

At a first time, a metal plate is placed at a distance of 8 metres. An example of the received signal is shown in figure 13. The first pulse in the received signal corresponds to the leakage between the transmitting/receiving antennas. The second pulse corresponds to the reflection on the obstacle. The correlation with the reference signal is presented in figure 14. The distance calculation gives a distance corresponding to 8.04 m instead of 8 meters, which is a very close fit.

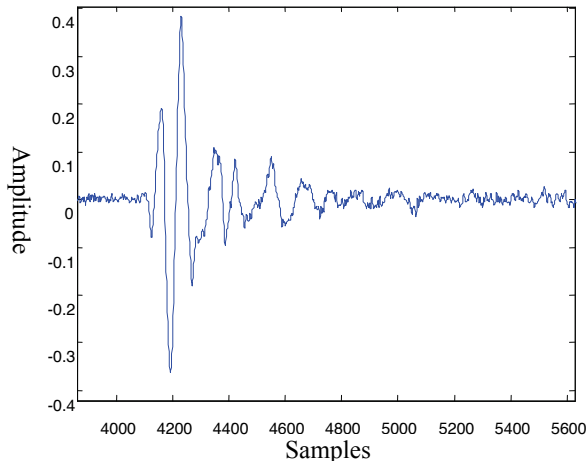


Fig. 12. Reference signal.

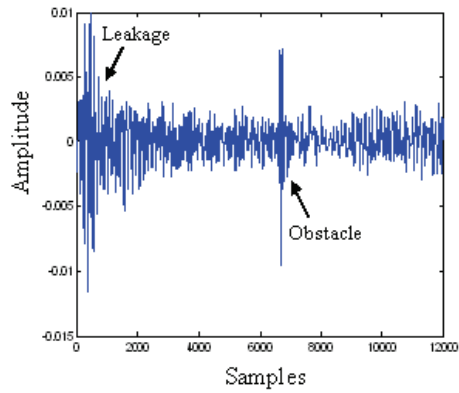


Fig. 13. The reflected echo by the metal plate placed at 8 m.

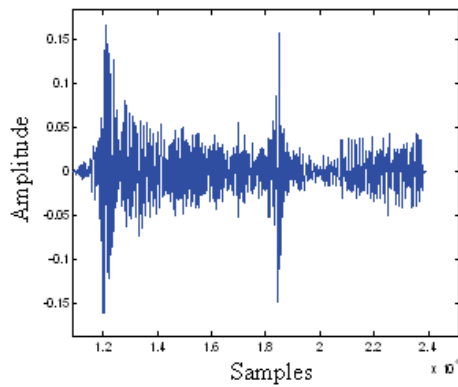


Fig. 14. Correlation signal result.

Then a car is placed at 10 metres in front of radar. The received signal and the calculation of correlation are presented respectively in figure 15 and 16.

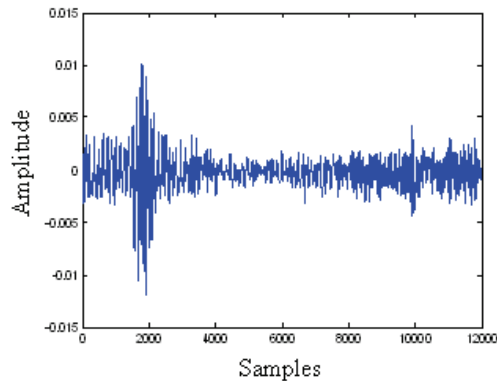


Fig. 15. Received echo reflected by car located at 10 m.

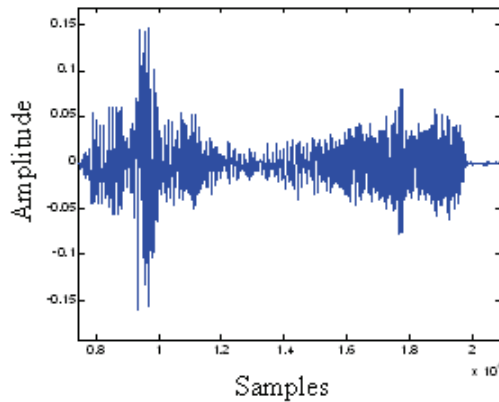


Fig. 16. Correlation signal.

The calculated distance obtained is 10.04 metres versus 10 metres theoretical; the calculated value is again very close to the real distance.

In order to place this radar in real road conditions, measurements involving a motorway barrier and a pedestrian are performed. First a motorway barrier is placed at 2.70 meters far from radar, the received signal is presented in figure 17 and the correlation is shown in figure 18.

The distance calculated using the developed radar is 2.85m, very near to the real distance of 2.70 m.

The reflected signal on pedestrian, placed at 2 meters, is presented in figure 19. The correlation signal is presented in figure 20.

The found distance is 1.87 metre for a real distance equal to 2 metres.

These previous measurements show that the developed UWB radar offers a great precision when using a single obstacle.

In addition, it is interesting to verify that the UWB radar is able to detect several obstacles at the same time with a good precision.

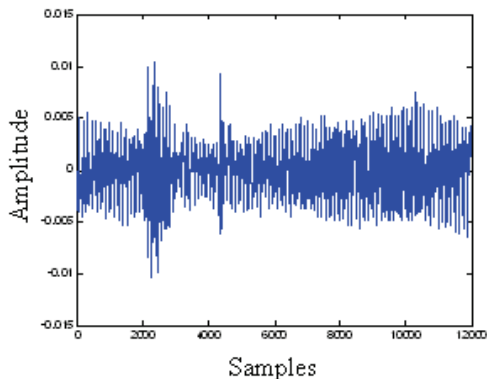


Fig. 17. Received echo in the case of a motorway barrier placed at 2.70 m.

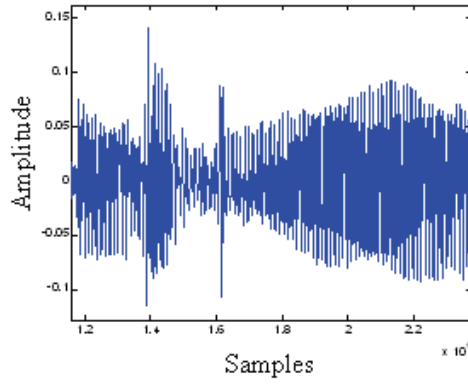


Fig. 18. Correlation signal.

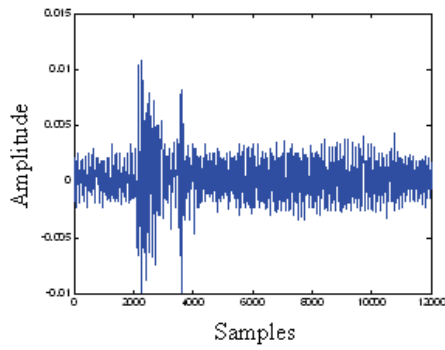


Fig. 19. Reflected signal by pedestrian placed at 2 m.

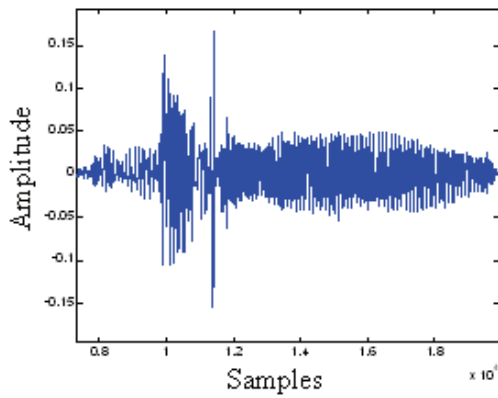


Fig. 20. Correlation signal using a pedestrian at 2 m far from radar.

## 7.2 The multiple obstacles detection case

A car is placed at 5 meters far from radar, a metal plate at 3 meters and a pedestrian at 1.70 meter.

On the received signal, presented in figure 21, the leakage signal between the antennas and the three echoes corresponding to the three obstacles can be distinguished easily. The corresponding correlation result is presented in figure 22.

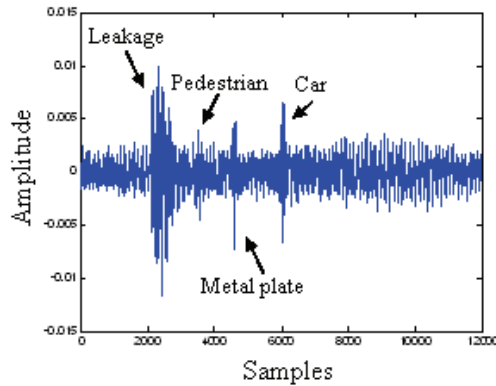


Fig. 21. Reflected echo by a metal plate, a car and a pedestrian.

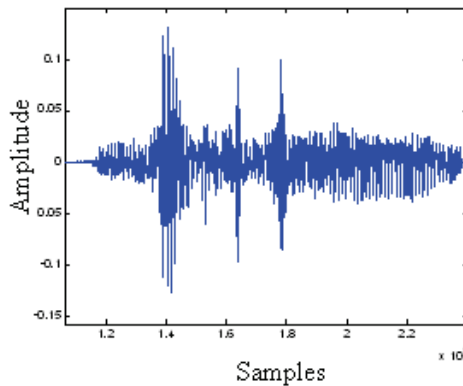


Fig. 22. Correlation signal.

A table comparing the real distances and those calculated is presented below (Table 1).

After processing the received signals, we notice that the UWB radar system offers a good precision in distance calculations.

However, we see that the correlation does not allow the automatic detection by the threshold method. In fact the correlation peak is drowned in the noise and the secondary lobes. It seems difficult to distinguish between the obstacle peaks and noise.

Obstacles	Real distance (m)	Calculated distance (m)	Precision (m)
Car	5	4.99	0.01
	10	10.04	0.04
Metal plate	3	2.88	0.12
	8	8.04	0.04
Pedestrian	1.70	1.57	0.13
Motorway barrier	2.70	2.85	0.15

Table 1. Distances comparisons

In order to solve this problem and to allow automatically detection, the High Order Statistics will be used. So to improve the detection performances of our system we look for new delay estimation algorithms. The concerned algorithms are based on the High Order Statistics. They give more performances than correlation (2<sup>nd</sup> statistics order) where the noises of the two distinct sensors are correlated. Detection is done by applying the algorithms to the two signals received by the two sensors.

In this study, to make detection we have only the received signal, our motivation to use the H.O.S (over 3) is in their capacities of the suppression of the Gaussian noise received attached to the useful signal. So, higher orders cumulants remove the Gaussian noise and keep the useful signal. These algorithms must be compatible with a use in real-time, which imposes operational limits of resource memory and in computing times, for this reason that we limit this study to the 4<sup>th</sup> order.

The expression of this algorithm is [Tugn1993]:

$$J_4(i_0) = \frac{\text{cum}_4(c(i-i_0), c(i-i_0), r(i), r(i))}{\sqrt{|\text{cum}_4((c(i), c(i)))| \cdot |\text{cum}_4(r(i), r(i))|}}$$

With:

c: is the reference signal

r: is received signal

$i_0$ : the decision time index

$$\text{cum}_4(c(i-i_0), c(i-i_0), r(i), r(i)) = \frac{1}{N} \sum_{i=0}^{N-1} c^2(i-k).r^2(i) - \left[ \frac{1}{N} \sum_{i=0}^{N-1} c(i-i_0).r(i) \right]^2 - \left[ \frac{1}{N} \sum_{i=0}^{N-1} c^2(i-i_0) \right] \left[ \frac{1}{N} \sum_{i=0}^{N-1} r^2(i) \right]$$

This algorithm is based on the assertion that the noise is Gaussian; its cumulants of order 4 is zero.

The result of these algorithms applied to the signal shown in figure 21 is shown in figure 23. The result of the algorithms Tugnait 4, compared with those of the correlation for the same signal (figure 22), gives performances much better. In fact, these algorithms make well leave the obstacles peaks from the noise. For that these algorithms will be much useful for automating the device.

Ongoing works show the capacity of this radar to identify the types of obstacles detected, thanks to the radar signature. So, this radar, has the capacity to detect not only single obstacle with a great precision, but also is able to distinguish obstacles in case of several obstacles.

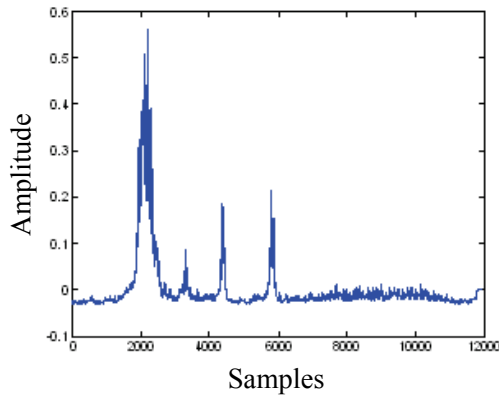


Fig. 23. The Tugnait 4 algorithms result

This study will be completed by establishing a database composed by recurrent obstacles signatures. This database could be obtained by elaborating correlation forms for different obstacles cases (metal, wood, pedestrian, wall...). Next step consists in developing signal processing algorithms able to perform automatic recognition by classification.

## 8. Conclusion

In this chapter, an original radar based on the new Ultra Wide Band technology is presented. This radar will be embedded on vehicles in order to increase road safety. We show the interest of this type of radar, thanks to the high degree of accuracy it offers and to its capacity to make the difference between various obstacles (cars, plates, pedestrians...). This study will be supplemented by a realization of the receiver and a method of adequate detection allowing the database classification of the obstacles, thanks to the UWB radar signature. This functionality allows better information to the driver or a follow-up of trajectory in the case of an automatic control application (Autonomous Cruise Control).

## 9. References

- [Bar2000] Barret, T. W. "History of Ultra Wide Band (UWB) radar & communications: pioneers and inventors", Progress in Electromagnetics Symposium 2000, Cambridge, MA, July 2000
- [Cham1992] Chambers,C.,S. R.Cloude and P. D. Smith (1992) "Wavelet processing of Ultra-WideBand radar signals", IEE Colloquium on Antenna and Propagation Problems of Ultra WideBand Radar, London, UK, 4p.
- [Carl2000] Carlberg, T.: «Analysis of Ultra Wide Band (UWB) technology for indoor geolocation and physiological monitoring system », Master Thesis, Chalmers University of Technology (Sweden), 2000
- [Dam2007] Damien Scherrer «OFCOM Infomailing N° 8», Federal Office of COMmunication, pp.11-15, September 2007

- [Elb2001] Elbahhar, F. Rivenq-Menhaj, A. Rouvaen, J.M. Deloof, P. and Boukour, T. «An Ultra-Wide band system for vehicle-to-vehicle communication», Proc. ITS Conf. (on CD-ROM), Sydney, Australia, Sept. 2001.
- [Elb2005] Elbahhar, F. Rivenq-Menhaj, A. Rouvaen, J.M, «Multi-user Ultra Wide Band communication system based on modified Gegenbauer and Hermite functions », Wireless Personal communications, Volume 34, Issue 3, August 2005
- [ESaf2006] The 28 eSafety recommendations, eSafety Compendium, pp. 44-45, May 2006
- [Fcc2002][http://www.fcc.gov/Bureaus/Engineering\\_Technology/Orders/2002/fcc02048.pdf](http://www.fcc.gov/Bureaus/Engineering_Technology/Orders/2002/fcc02048.pdf)
- [Fcc2000] Federal Communication Commission. « Notice of proposed rule making », FCC 00-163, Et Docket 98-153, In the matter of revision of part 15 of the commission's rules regarding Ultra wideband transmission system, Washington, 11 may 2000.
- [Lach2002] Lachlan, B.M. Ghavami, M. and Kohnno, R. «Multiple Pulse Generator for Ultra-Wideband Communication using Hermite Polynomial Based Orthogonal Pulses », IEEE Conference on Ultra Wideband Systems and Technology, 2002.
- [Tay1995] Taylor, James D. t al introduction to Ultra Wideband radar system, James D. Taylor Editor, CRC Press, Boca Raton, 1995, 670 p.
- [Tugn1993] J. K. Tugnait. Timr delay estimation with unknow spatially correlated gaussian noise. IEEE, Transaction on signal processing, vol. 42, n° 2, pages 549-558, Febrary 1993.



## **Radar Technology**

Edited by Guy Kouemou

ISBN 978-953-307-029-2

Hard cover, 410 pages

**Publisher** InTech

**Published online** 01, January, 2010

**Published in print edition** January, 2010

In this book “Radar Technology”, the chapters are divided into four main topic areas: Topic area 1: “Radar Systems” consists of chapters which treat whole radar systems, environment and target functional chain. Topic area 2: “Radar Applications” shows various applications of radar systems, including meteorological radars, ground penetrating radars and glaciology. Topic area 3: “Radar Functional Chain and Signal Processing” describes several aspects of the radar signal processing. From parameter extraction, target detection over tracking and classification technologies. Topic area 4: “Radar Subsystems and Components” consists of design technology of radar subsystem components like antenna design or waveform design.

### **How to reference**

In order to correctly reference this scholarly work, feel free to copy and paste the following:

L. Sakkila, C. Tatkeu, Y. ElHillali, A. Rivenq, F. ElBahhar and J-M. Rouvaen (2010). Short Range Radar Based on UWB Technology, Radar Technology, Guy Kouemou (Ed.), ISBN: 978-953-307-029-2, InTech, Available from: <http://www.intechopen.com/books/radar-technology/short-range-radar-based-on-uw-technology>

# **INTECH**

open science | open minds

### **InTech Europe**

University Campus STeP Ri  
Slavka Krautzeka 83/A  
51000 Rijeka, Croatia  
Phone: +385 (51) 770 447  
Fax: +385 (51) 686 166  
[www.intechopen.com](http://www.intechopen.com)

### **InTech China**

Unit 405, Office Block, Hotel Equatorial Shanghai  
No.65, Yan An Road (West), Shanghai, 200040, China  
中国上海市延安西路65号上海国际贵都大饭店办公楼405单元  
Phone: +86-21-62489820  
Fax: +86-21-62489821

© 2010 The Author(s). Licensee IntechOpen. This chapter is distributed under the terms of the [Creative Commons Attribution-NonCommercial-ShareAlike-3.0 License](#), which permits use, distribution and reproduction for non-commercial purposes, provided the original is properly cited and derivative works building on this content are distributed under the same license.